small
NANO MICRO

Three-Dimensional Electrospun Alginate Nanofiber Mats via Tailored Charge Repulsions

*Christopher A. Bonino, Kirill Efimenko, Sung In Jeong, Melissa D. Krebs, Eben Alsberg, and Saad A. Khan**

The formation of 3D electrospun mat structures from alginate–polyethylene oxide (PEO) solution blends is reported. These unique architectures expand the capabilities of traditional electrospun mats for applications such as regenerative medicine, where a scaffold can help to promote tissue growth in three dimensions. The mat structures extend off the surface of the flat collector plate without the need of any modifications in the electrospinning apparatus, are self-supported when the electric field is removed, and are composed of bundles of nanofibers. A mechanism for the unique formations is proposed, based on the fiber–fiber repulsions from surface charges on the negatively charged alginate. Furthermore, the role of the electric field in the distribution of alginate within the nanofibers is discussed. X-ray photoelectron spectroscopy is used to analyze the surface composition of the electrospun nanofiber mats and the data is related to cast films made in the absence of the electric field. Further techniques to tailor the 3D architecture and nanofiber morphology by changing the surface tension and relative humidity are also discussed.

1. Introduction

Electrospinning is a facile method to fabricate nanofibrous mats, which have a range of applications. The feature sizes of electrospun mats, such as fiber diameters, can be tailored by the solution properties (e.g., viscosity, polymer concentration) and process conditions (e.g., flow rate, electric field).[1] The mat thickness is also affected by the total mass of deposited fibers and size of the collector plate. As the mat thickness is much smaller than the mat diameter, it is commonly used in applications benefiting from two-dimensional (2D), porous structures. For example, electrospun mats have been used as filters,[2] battery electrodes,[3] and separators.[4] In these applications, a high surface-area material with a small thickness (<100 μm) may be desirable, because of the size constraints of the testing media. However, for other applications (i.e., tissue engineering) a 2D mat is less ideal. One role of a tissue scaffold is to mimic the extracellular matrix, a fibrous 3D network that provides structural support for developing tissues.[5] Although electrospun mats have shown promise as tissue scaffolds,[6] their feature sizes and topography also have drawbacks. Specifically, electrospun nanofiber mats have a relatively flat topography, limited thickness, and dense fiber packing; as such, when used as tissue scaffolds, cell infiltration can be restricted to the top layers of the electrospun mat (e.g., Bhattarai et al.[7]). Hence, without modification, a traditional electrospun nanofiber mat may have limited use in regenerative medicine.

Electrospun mat formations have been tailored by a variety of approaches in order to expand their capabilities.

Dr. C. A. Bonino,[+] Prof. K. Efimenko, Prof. S. A. Khan
Department of Chemical & Biomolecular Engineering
North Carolina State University
Raleigh, NC 27695, USA
E-mail: khan@eos.ncsu.edu
Dr. S. I. Jeong, Dr. M. D. Krebs, Prof. E. Alsberg
Department of Biomedical Engineering
Case Western Reserve University
Cleveland, OH 44106, USA
Prof. E. Alsberg
Department of Orthopaedic Surgery
Case Western Reserve University
Cleveland, OH 44106, USA
[+] Current address: RTI International, Research Triangle Park, NC 27709, USA

DOI: 10.1002/smll.201101791

One such route has been to modify the electrospinning setup. Changes to the collector plate, which vary in complexity from parallel plates[8] and screws,[9] to other custom-built fixtures,[10,11] have led to controlled arrangements of fibers in 2D and 3D mat structures. In addition, inert particle spacers (e.g., salts)[12,13] and micrometer-sized fibers[14,15] have been introduced during electrospinning to increase the void space between nanofibers. The mat porosity has also been manipulated by post treatments of the conventional electrospun mats, such as photomasking[16] or stacking layered mats.[17] Although these approaches may be novel, they add additional process steps and/or accessories, and some may have challenges associated with preserving the mat architecture during removal from the collector.

An alternative approach to making 3D mat structures, which has received little attention, focuses on the initial formulation of the electrospun solution. Careful selection of the solution components and properties may lead to arrangements of electrospun fibers that extend outward from the surface of the collector plate (3D structures).[13,18] These 3D formations can be accomplished by fabricating fibers containing a high charge density material (i.e., a polyelectrolyte) with the charges distributed on or near the outer surfaces, thus creating repulsive forces between adjacent fibers.

The applied electric field during electrospinning can have significant consequences on the distribution of charged solution components in the formed fibers. The movement of an ionic species within a DC electric field is influenced by a variety of forces (e.g., Coulombic, electrophoretic).[19] In one predominant outcome, a negatively charged (macro) molecule can be directed towards the positive polarity of the electric field source. During electrospinning the negatively charged species can be preferentially driven to the Taylor cone and electrospun jet surfaces.[20] This phenomenon can be exploited to prepare electrospun fibers with tailored surface compositions. For example, Sun et al. electrospun a solution containing neutral (i.e., polyethylene oxide (PEO)) and charged (i.e., peptide-polymer conjugate) components, and observed that the charged peptide populated the outer surfaces, whereas PEO was found within the fiber interiors.[21] Thus, electrospinning solutions with ionic components can produce fibers with charged surfaces.

In addition to the solution's ionic conductivity, the relative humidity is another variable that has significant effects on electrospinning. Humidity has been linked to the creation/suppression of bead defects,[22] as well as porous surfaces,[23,24] in electrospun fibers. For water-soluble polymers, reducing the humidity raises the rate of solvent evaporation, which causes the electrospun jet to solidify at a closer distance to the source (needle).[25] The solidified jet no longer retains its viscoelastic behavior nor its ability to be elongated or subjected to additional capillary instabilities. Thus, water-soluble fibers electrospun at low humidities (<20%) can have larger diameters and fewer bead defects than at high relative humidity (RH) conditions (>40%).[22] Despite the implications on fiber morphology, few electrospinning studies typically report the RH, much less the control ambient experimental conditions. Variations in lab environments may hamper the reproducibility of results caused by the week-to-week variations in the same lab, or between labs in different parts of the world.

In this study, not only do we control the humidity, we also use it to manipulate the formation of 3D structures in electrospun fiber mats. Polyelectrolytes forming solid substrates (i.e., films) can be hydrated by water from a humid ambient atmosphere, leading to the solvation and higher mobility of the ions.[26] Thus, by changing the humidity of the electrospinning conditions, we alter the concentration of dissociated ions in the fibers, which affects the like-charge repulsions between fibers and drives the 3D mat formation.

A few studies have reported the occurrence of 3D electrospun mats from solutions containing charged species (e.g., salts,[27] polyelectrolytes[13,18]). However, the proposed mechanisms failed to address the influence of the positively charged electric field at the needle source on negatively charged solution components. In this work, we prepare electrospun fibers that contain sodium alginate, an anionic polyelectrolyte that has been shown to display electroresponsive behavior[28] in DC fields. We propose that negatively charged groups (i.e., carboxylic acid) on alginate populate the surfaces of the electrospun fibers aided by the attractive forces in the applied field. The resulting fibers have predominately negatively charged surfaces, and experience repulsion from other charged, adjacent fibers, causing them to extend away from the collector plate. This phenomenon can be manipulated by the number of disassociated ions within the fiber, which is affected by the moisture content of the fibers, by way of the RH. To our knowledge, we are the first to methodically alter the formation of 3D electrospun structures using this approach. The 3D mats in this work have fascinating architectures, which could find use in many applications, such as regenerative medicine. Our 3D structures contain alginate, a natural biocompatible polysaccharide, as well as PEO and Pluronic F127 (an ethylene oxide(EO)/propylene oxide (PO) block copolymer), both Food and Drug Administration (FDA)-approved polymers, which make the resultant scaffolds promising for biomedical applications.

2. Results and Discussion

2.1. Formation of 3D Electrospun Mats

We have observed 3D mat structures during the electrospinning of solutions containing alginate (M_W 37 kDa) and PEO (M_W 600 kDa), with and without Pluronic F127 nonionic surfactant. We believe that the chemical structure of alginate, which contains carboxylic acid groups that can dissociate into negatively charged ions, contributes to like-charge Coulombic repulsions. As a result, alginate-based fibers are repelled by neighboring fibers and create a 3D mat structure. One example of a 3D structure is shown in **Figure 1**a. This mat was formed by electrospinning an aqueous alginate–PEO–Pluronic F127 blend (10.6:0.8:1.5 wt%) for 40 minutes (0.5 mL h^{-1}) at 23 °C and 30% relative humidity. A cone-like formation extends about 7 cm off the surface of the collector plate towards the needle. Smaller peaks (<1 cm tall) surround the 3–4 cm wide base of the larger cone. Peaks also

small 2012,
DOI: 10.1002/smll.201101791

small NANO MICRO

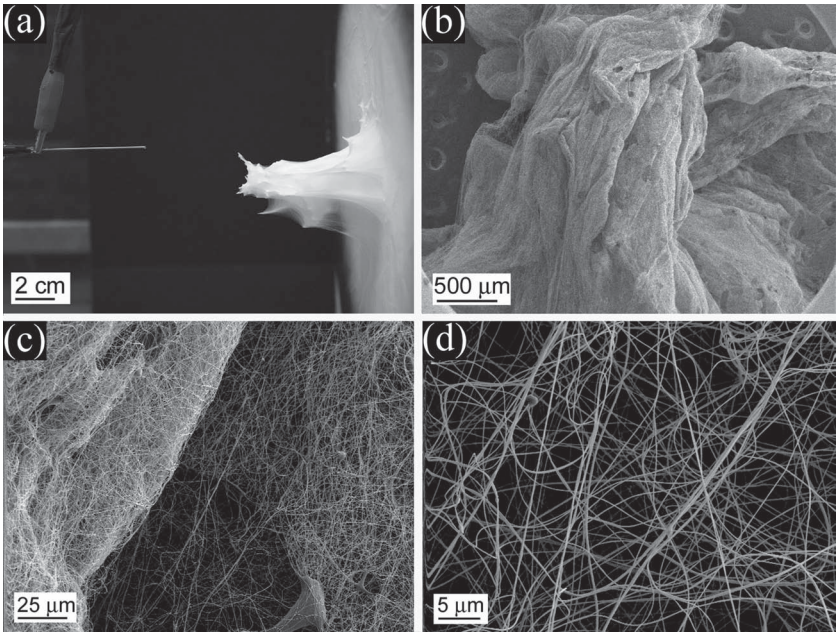

Figure 1. a) Photograph and b–d) SEM images of electrospun cone formation, composed of layers of nanofibers. The electrospinning solution contained: alginate–PEO–F127 (10.6:0.8:1.5 wt%) in water (23 °C, 30% RH).

protrude from the cone tip and along the underside of the cone (near the bottom of the photograph). Bundles of fibers span between the peaks and the cone base, which are oriented parallel along the 3D structure, and perpendicular to the collector plate. Interestingly, the cone structure remains fixed in place after removing the electric field. The ability of the 3D mat structure to support its own weight together with the use of a conventional collector system, makes this a desirable approach from the perspective of possible mat damage associated with the removal from a complex collector plate configuration (e.g., screws extending from the plate[9]). Furthermore, the 3D structure is significantly taller than conventional nanofiber mats, which are typically less than 100 µm thick[29] after several hours of electrospinning. To our knowledge, we are one of the first to report the occurrence of a self-supporting 3D electrospun mat.

Examination of the 3D mat with scanning electron microscopy (SEM) reveals that the cone tip has an asymmetrical appearance, consisting of several folds that run along the direction of its growth (Figure 1b). Furthermore, the cone is composed entirely of layers of nanofibers (Figure 1c,d). Nanofibers located at the base and pinnacle of the cone have similar diameters: 221 ± 31 and 249 ± 45 nm, respectively. This result was surprising to us, considering that the distance that the electrospun jet travels from the needle to the cone tip or base varies from 5 to 12 cm, corresponding to different amounts of stretching in the whipping instability region. This result suggests that most of the solvent evaporated and the jet solidified within a short distance of the needle, which may have prevented the jet from experiencing further elongations and fiber diameter reductions. Additionally, the fibers shown in Figure 1c,d have few bead defects. The occurrence of bead defects is affected by the solution surface tension and ambient RH, and will be addressed in detail later.

The formation of the 3D structure was investigated as a function of time to gain a better understanding of its growth mechanism. The peak formation on the electrospun mat shown in **Figure 2**a occurs after 9 minutes with individual feature sizes on the order of 1 mm, which is on the threshold of detection by the naked eye. A textured appearance is more prominent in the center of the mat compared to the outer perimeter. SEM analysis of the formed structures revealed dense groupings of nanofibers, the largest of which are about 150 µm across and are on top of a base layer of fibers (Figure 2d,g,j). Holes or craters in the mat surface can be attributed to capillary instabilities, which caused the breakup of the jet[30] into droplets.

We hypothesize that, after 9 min of electrospinning, the base layer of fibers prevented surface charges on the topmost fibers from being neutralized by the grounded collector plate. We further speculate that repulsions from excess negative surface charges between adjacent fibers cause fiber sections to extend from the surface of the mat as schematically depicted in **Figure 3**a. Repulsive forces between nearby fibers have been previously shown[31] to occur with traditional electrospun mats, as well. Additional layers of fibers that are deposited onto the mat are also repelled from the site of the protrusion, causing a peak to form. As the peak height increases, the spatial distribution of the electric field between the needle and plate also changes. Compared to the flat surface in a traditional electrospun mat, the peaks create differences in the topography across the mat, and cause localized regions of a higher electric field. As a result, subsequent layers of fibers are preferentially deposited in the vicinity of the peaks. Several fibers, centered on one peak (left side of image, Figure 2d), also extend between other nearby peaks and form lines of parallel fibers. The arrangement of uniaxially aligned fibers has been previously reported[8,32] as the lowest energy configuration for groups of highly charged fibers, as a result of Coulombic repulsions. Additional layers of fibers with negatively charged surfaces are continuously deposited near the peak sites, which cause the peaks to become more pronounced.

After 15 minutes, the largest peaks extend >1 cm off the surface of the collector plate (Figure 2b). Furthermore, some of the smaller formations have evolved from disordered bundles of fibers that are about 50 µm tall to peaks with defined features of about 200 µm tall (Figure 2e). Layers of fibers connect the neighboring peaks, creating the ridges around the peak formations. Fibers that are not in the right position to connect the neighboring peaks are deposited randomly over the ridges (Figure 2h). The peaks are composed entirely of nanofibers (Figure 2k), which suggest that the dynamics of the 3D mat formation occur after the jet has been elongated to its final dimensions. Therefore, the combination of

DOI: 10.1002/smll.201101791

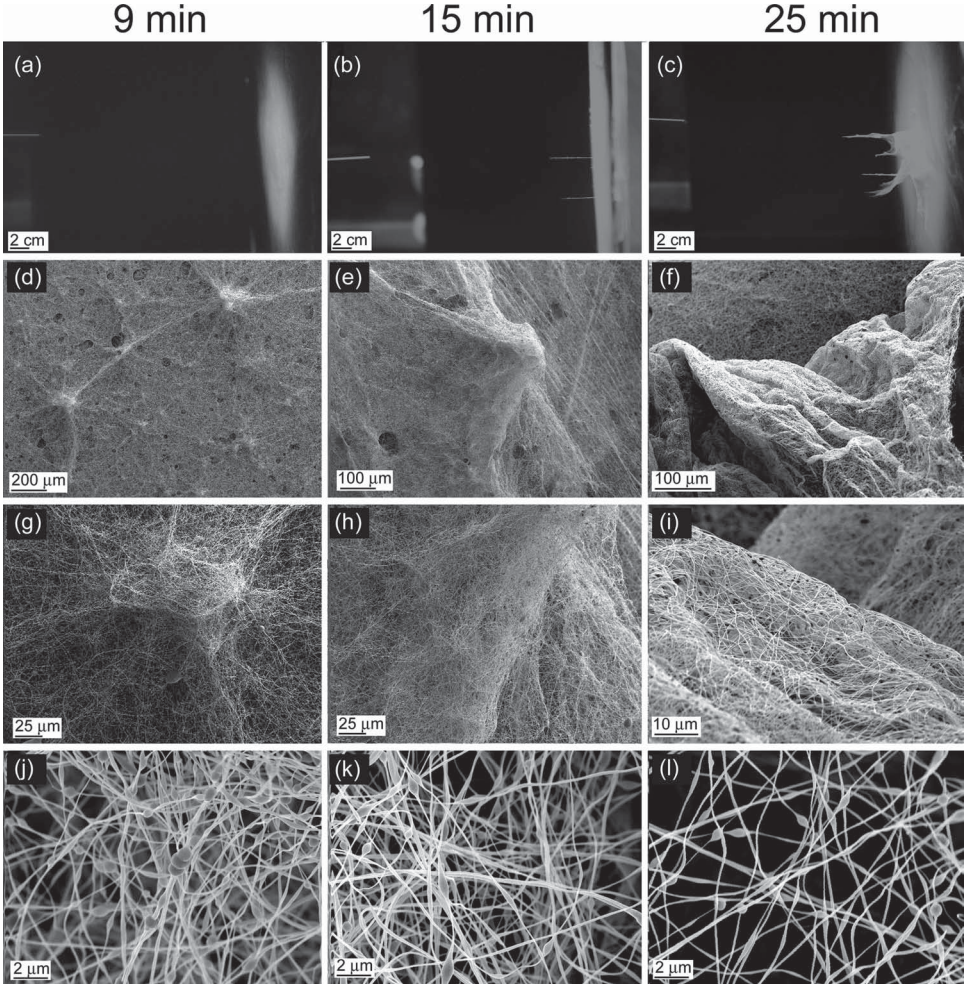

Figure 2. a–c) Photographs and d–l) SEM images of the formation of a 3D mat structure after 9 (a,d,g,j), 15 (b,e,h,k), and 25 min (c,f,i,l) of electrospinning an aqueous alginate–PEO–F127 (10.6:0.8:1.5 wt%) solution (23 °C, 40% RH).

the electric field and the surface charges on the fibers alters their positions on the mat.

The 3D structures developed into macroscale formations after 25 minutes (Figure 2c). Centimeter-sized peaks, connected by layers of fibers, made up the base of the structure that is 5–7 cm across. Figure 2f shows that the mat has a complicated structure with ridges and valleys (10–100 µm wide). Topography on this scale may be advantageous if used as a scaffold for tissue engineering, as cells (which, when rounded, are roughly on the order of 10 µm) would be able to move into these spaces. Figure 2i and l show the structures at different magnifications revealing the presence of nanofibers. A movie of the 3D mat structure forming off the collector plate is included in the Supporting Information.

Overall, the 3D structures have good repeatability. Duplicate experiments using the same solution composition and ambient conditions yield 3D structures with comparable formation dynamics, fiber morphologies, and mat appearances (see Figure S1 and Table S1 in the Supporting Information).

As a result of these experimental observations, we hypothesize that the 3D mechanism is based on the repulsions between neighboring fibers from the charged groups (i.e., carboxylic acid) in alginate. In addition, we believe that the concentration of the negatively charged groups is disproportionately distributed throughout the fiber, favoring the outer surfaces, as a result of the electric field. The interplay between the applied electric field and repulsions between charged species influences the dynamics of the entire electrospinning process, from the spinneret[21] to the collector plate.[30,31] As the polymer solution passes through the needle that is connected to the power supply, negatively charged species are attracted to the positively charged electric field on the needle walls, as well as the Taylor cone outer surfaces (Figure 3b).[20] In turn, alginate becomes concentrated near the solution–air interface of the electrospun jet and the resulting nanofibers, whereas PEO remains within the interior (Figure 3a).

X-ray photoelectron spectroscopy (XPS) confirmed our hypothesis. Scans of the pure materials show that alginate and PEO have different atomic compositions of oxygen and carbon, 40.3:53.9 and 31.5:68.0, respectively (**Table 1**a and Figure S2 (Supporting Information)). (Sodium is unique to the alginate of the materials in this study.) In addition to the pure materials, we also analyzed films and electrospun mats containing alginate–PEO (10.6:0.8 wt%) without the Pluronic surfactant, in order to investigate the surface segregation of the alginate–PEO polymer blend. Analysis of a

DOI: 10.1002/smll.201101791

small NANO MICRO

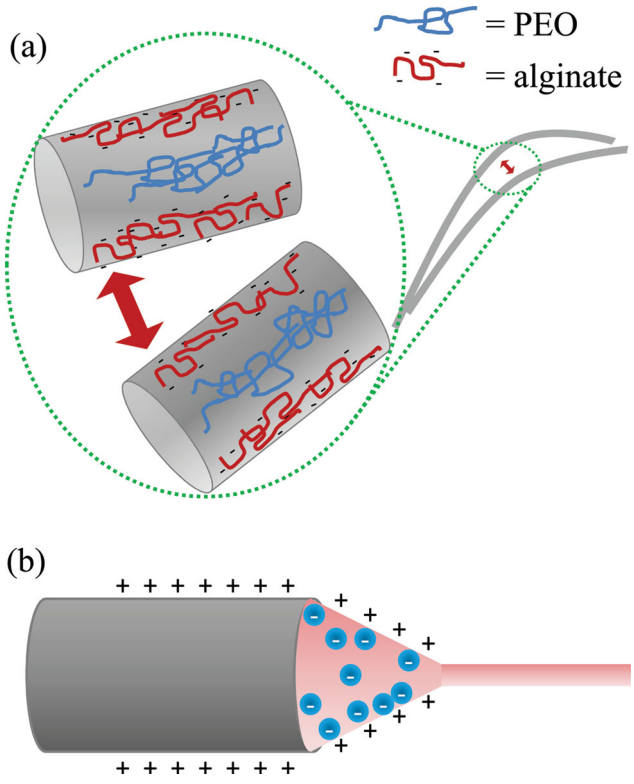

Figure 3. The formation mechanism of 3D electrospun mats is attributed to Coulombic repulsions between neighboring electrospun fibers. a) Fibers containing negatively charged alginate chains on their outer surfaces are pushed apart by like-charge repulsions. b) During electrospinning, alginate is preferentially directed to the surface of the Taylor cone and jet by the applied, positive-polarity electric field source. PEO, a neutral polymer, remains predominantly within the interiors of the electrospun jet and fibers.

solvent-cast film of the alginate–PEO blend reveals that the atomic concentration within 5–10 nm from the top surface matches that of PEO. In a thermodynamically stable polymer blend, the more hydrophobic polymer preferentially segregates to the air interface. In contrast, the C and O composition of the outer surface of the electrospun nanofibers practically matches that of alginate. (The presence of sodium might be related to 'bound' counter ions[33] in the vicinity of the charged polyelectrolyte.) Thus, the electric field influenced the spatial composition within the fibers, resulting in the negatively charged polyelectrolyte dominating the surface composition.

2.2. Effects of Surfactants on 3D Electrospun Mat Formation

A nonionic surfactant is critical to the 3D mat formation and fiber morphology. For the latter, the connection between reducing the surface tension in electrospinning solutions and the suppression of bead defects are well documented.[7,34] We recently showed that a PEO-based nonionic surfactant, Pluronic F127, helped mitigate the formation of beads in alginate–PEO blends.[35] In this study, Pluronic F127 also aids in the 3D mat formation. Electrospun mats prepared from alginate–PEO (10.6:0.8 wt%) solutions have minimal 3D topography as compared to mats from solutions containing 1.5 wt% F127 in the same conditions, as shown in **Figure 4**a and **Figure 5**g, respectively. However, SEM analysis reveals that small peaks about 20–50 μm across are present on the mats even without the surfactant, which validates our central hypothesis about like-charge repulsions (Figure 4b). The addition of Pluronic F127 lowers the surface tension of the alginate–PEO solution from 57 to

Table 1a. Surface atomic composition measured by XPS.

	Peak position [eV]	PEO [%][a,b]	Alginate [%][a,c]	Alginate-PEO[d] Film[b] [%][a]	Alginate-PEO[d] Electrospun Mat [%][a]
O	532	31.5	40.3	29.6	38.7
C	286	68.0	53.9	64.8	56.9
Na	1070	0	5.8	2.8	4.2
Si[f]	151	0.4	0	2.8	0.2

[a]Atomic percentage is the average of at least two runs, standard deviation <2.5%; [b]Solvent cast film; [c]Neat material; [d]Solution blend 10.6:0.8 wt% (93:7%); [e]Solution blend 10.6:0.8:1.5 wt%; [f]Silica is present in PEO in the form of fumed silica.

Table 1b. Surface atomic composition measured by XPS, with Pluronic F127 surfactant.

	Peak position [eV]	PEO [%][a,b]	Alginate [%][a,c]	Pluronic F127 [%][a,c]	Alginate-PEO-F127[e] Film[b] [%][a]	Alginate-PEO-F127[e] Electrospun Mat [%][a]
O	532	31.5	40.3	20.7	28.0	32.5
C	286	68.0	53.9	79.3	69.0	65.4
Na	1070	0	5.8	0	2.5	1.7
Si[f]	151	0.4	0	0	0.6	0.5

[a]Atomic percentage is the average of at least two runs, standard deviation <2.5%; [b]Solvent cast film; [c]Neat material; [d]Solution blend 10.6:0.8 wt% (93:7%); [e]Solution blend 10.6:0.8:1.5 wt%; [f]Silica is present in PEO in the form of fumed silica.

DOI: 10.1002/smll.201101791

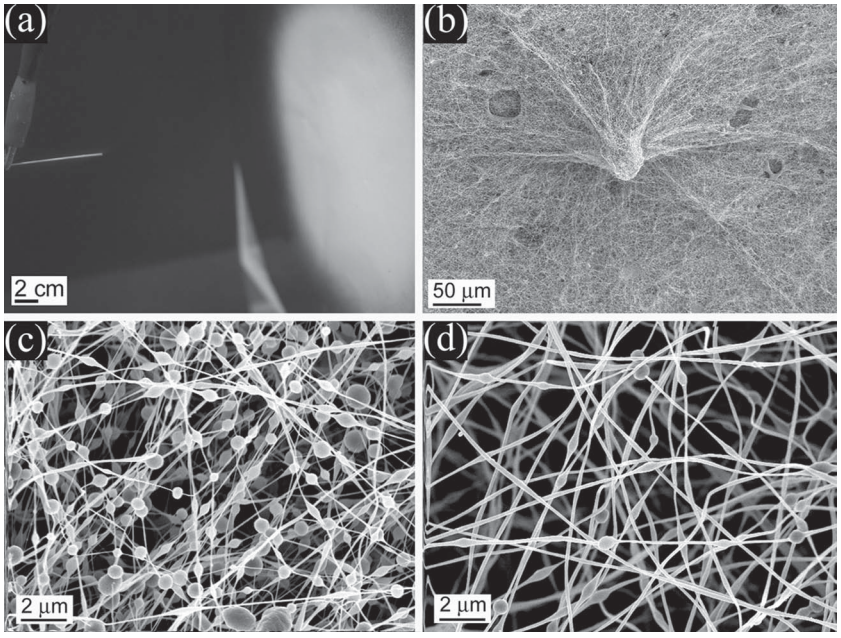

Figure 4. a) Photograph of electrospun mat with 2D visual appearance prepared from a surfactant-free solution containing alginate–PEO (10.6:0.8 wt%) at 23 °C, 40% RH. b,c) SEM images of peaks on the mat surface (b) and beaded nanofibers (c) prepared from the surfactant-free solution. d) SEM image of nanofibers prepared from the alginate–PEO solution containing Pluronic F127 surfactant (1.5 wt%).

35 mN m^{-1} (**Table 2**). We speculate that the reduction in surface tension allows for more alginate to migrate to the air–water interface with the applied electric field, as compared to the solution without the surfactant. XPS analysis of films and electrospun mats from solutions containing Pluronic F127 differ from those in solutions without surfactant (Table 1b and Table 1a, respectively). Specifically, the surface concentration of the electrospun mats does not match the atomic composition of alginate (O/C 40.3:53.9). As Pluronic contains a polypropylene oxide (PPO) block that is more hydrophobic than the other materials in the solution, it is present at the surface of both the films and the electrospun fibers. However, because the XPS is only sensitive to the top 5–10 nm of the sample, it is likely that the atomic composition measurement also includes other blend components. Based on the XPS results from the surfactant-free solutions, we believe that the film and electrospun surface compositions include Pluronic F127 with PEO, and Pluronic F127 with alginate, respectively.

2.3. Effects of Relative Humidity on 3D Electrospun Mat Formation

In addition to surfactants, humidity has a significant effect on fibers formed during electrospinning. As stated above, aqueous polymer solutions transition from uniform to beaded fibers as the humidity is increased.[22] Moreover, the effects of humidity make the electrospinning process even more complicated because of the presence of a polyelectrolyte component in the initial formulations. High humidities (>40%) can cause beaded fibers to form; moreover, the retained water in the fibers also causes the polyelectrolyte to dissociate into charged groups ($R\text{-}COO^-$, Na^+), raising its charge density. As a result, fibers can be reoriented by like-charge repulsions in adjacent fibers (as well as by the electric field) and can lead to a 3D mat structure. Thus, the relative humidity is a critical variable to manipulate the 3D structures in the electrospun mats.

Beginning at the low humidity condition (ca. 10%), only a small texture was visible by the naked eye on the surface of the mat. Analysis with SEM revealed that the mats contained uniform, bead-free fibers with average diameters of 300 ± 40 nm (Figure 5a,b). Increasing the humidity beyond 10% RH has profound effects on the mat appearance. At 20% RH, a conical structure (2 cm tall, 2 cm diameter) was limited to a small region of the collector plate, whereas surrounding regions lacked 3D structures (<1 mm peaks) (Figure 5c,d; **Table 3**). The cone formed relatively slowly as the first signs of peaks appeared after 30 min. With less water retained within the fiber in the dry environment, there are fewer dissociated carboxylic acid groups and charges on the outer surfaces of the fibers. Thus, neighboring fibers are repelled over shorter distances compared to fibers with greater concentrations of surface charges, and the 3D formation is a compact, slow-forming structure.

The 3D structure became much larger in diameter and height at 30% RH (Figure 5e,f). The structure also formed faster than under dryer conditions (1 cm tall in 10 min) because with more retained water, the alginate-based fibers had more surface charges. Despite the unique shape of the mat, the fibers were bead-free, with diameters of 237 ± 33 nm. Of all the conditions evaluated, the 3D mats prepared at 30% RH show a combination of uniformly sized fibers and large structural formation.

At 40–50% RH, the electrospun mat transitions to a new 3D formation (Figure 5g-j). Instead of a self-supporting cone, 0.5–2 cm wide strands form on the collector plate and align with the electric field. A similar observation was reported previously with another charged polymer (i.e., poly(*p*-xylene-tetrahydrothiophenium chloride),[18] which was attributed to the accumulation of excess charges on the sections of the electrospun fibers. Recent work by our group also identified a similar behavior with electrospun solutions containing polyethylene oxide and sodium chloride.[36] Each strand starts from the pinnacle of a peak on the collector plate. As we discovered with the cone structures, the strands are also composed of sub-micrometer diameter fibers (**Figure 6**a). One notable difference is that the strands contain clusters of fibers oriented perpendicular to the collector plate (or parallel to the electric field) (Figure 6b).

We hypothesize that increasing the humidity leads to an increase in the density of charges on the fiber surfaces. The

small 2012,
DOI: 10.1002/smll.201101791

small NANO MICRO

Table 2. Properties of electrospinning solutions evaluated for 3D mats.

	Alginate-PEO-F127[a)]	Alginate-PEO[b)]
Zero Shear Viscosity [Pa s]	4.3	4.2
Conductivity [mS cm^{-1}][c)]	13.2 ± 1.3	14.1 ± 1.4
Surface Tension [mN m^{-1}][c)]	35 ± 1	57 ± 1
Electrospinning Comments	3D mat	2D mat

[a)]Solution blend 10.6:0.8:1.5 wt%; [b)]Solution blend 10.6:0.8 wt%; [c)]Values are averages ± standard deviations of five measurements.

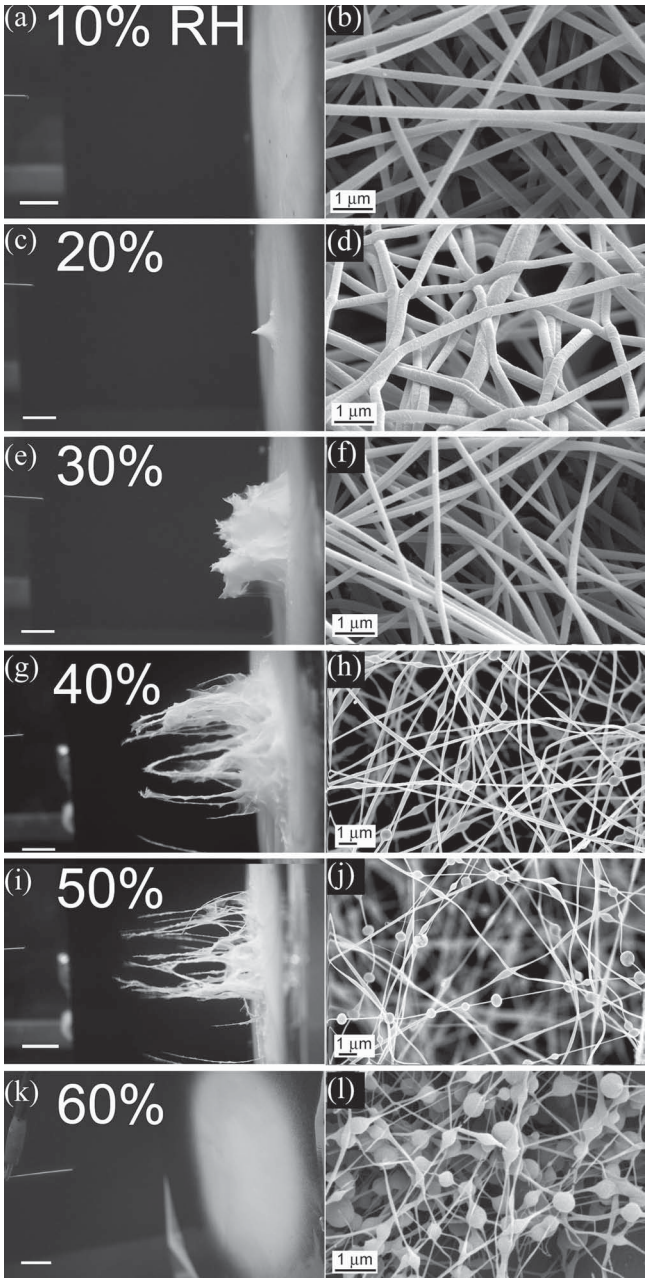

Figure 5. Photographs (a,c,e,g,i,k) and SEM images (b,d,f,h,j,l) of electrospun mat structures and nanofibers, respectively, prepared at six different relative humidity conditions by electrospinning an alginate–PEO–F127 (10.6:0.8:1.5 wt%) solution. The temperature was maintained at 23 °C. Each solution was electrospun for 40 minutes. The scale bars on the photographs are 2 cm.

like-charge repulsions between fibers result in parallel alignments, in order to minimize the electrostatic forces. The strands of fibers that are anchored to the mat surface at one point extend outward along the field lines. Subsequent layers of fibers are deposited on top of the aligned fiber clusters, which increase the size of the strand. In addition, bead defects are present on these fibers, which are consistent with water-soluble polymers electrospun in 40–50% RH.[22] Compared to the 3D structure at 30% RH, the strands formed at 40 and 50% RH are taller (up to 7 cm), and spread over a larger area on the mat (6 cm × 10 cm). However, the strands took longer to form than the cone structure, 16–18 min as opposed to 10 min, respectively (Table 3). We hypothesize that the 3D formation under high humidity conditions was distributed over a vast area on the collector plate as a result of the fibers' high surface charge densities. In addition, the size of the mat may be the result of large regions of whipping instabilities[34] that occur in a partially solidified jet. Thus, the 3D structure was distributed over a vast area, leading to a slower rate of formation compared to the 30% RH condition. Furthermore, the greater regions of whipping instabilities in the jet contributed to the formation of bead defects, as well as smaller fiber diameters.

At even higher RH (60%) the 3D structure did not form within 40 minutes of electrospinning. The 2D mat was composed of heavily beaded fibers, probably because of the whipping instabilities in the jet (Figure 5k,l). Humid conditions contribute to a high concentration of dissociated carboxylic groups at the fiber outer surfaces and the water vapor in the air may also cause charge screening, as well as a breakdown of the electric field.

The variety of 3D mat structures prepared under a range of humidity conditions can be customized for the desired use. The driest conditions are most suitable for uniform fiber diameters and relatively flat mat topographies, whereas cone and strand structures form at moderate humidity levels. High humidity levels are appropriate if alginate beads/spheres are preferred to fibers.

3. Conclusion

Blends of alginate and PEO, with and without Pluronic F127 surfactant, were electrospun into 3D formations composed of nanofibers. The formation of these 3D nanofibrous structures can be attributed to the polyelectrolytic nature of alginate and the electrospinning conditions. In particular, we explained the 3D structure as a result of repulsions between neighboring fibers, related to surface charges. We showed by XPS analysis that alginate, a negatively charged polyelectrolyte, is preferentially distributed on the outer surfaces of the electrospun fibers, whereas PEO preferentially surface-segregates in the absence of an electric field. The relative humidity changes the 3D structure, which we attribute to a greater number of surface charges from the dissociated alginate chains. This approach to making 3D nanofibrous architectures from solutions containing charged components is a strategy to expand the capabilities of electrospinning beyond traditional 2D mat structures. For instance, the more porous

DOI: 10.1002/smll.201101791

Table 3. Observations of electrospun formations at various relative humidities.

Relative Humidty	10%	20%	30%	40%	50%	60%
Time for 1 mm tall formation [min][a)]	–	30	5	12	17	–
Time for 1 cm tall formation [min][a)]	–	35	10	16	18	–
2D mat diameter [cm]	14	14	17	17	16	16
3D mat diameter [cm][b)]	–	2	6	7–10	6–10	–
3D mat height [cm]	<0.1	2	5	7	7	<0.1
Average fiber diameter [nm][c)]	300 ± 40	294 ± 44	237 ± 33	239 ± 41	171 ± 40	80 ± 23
Comments on mat	textured appearance	small cone	wide cone	strands	strands	textured appearance
Comments on fibers	uniform diameters	uniform diameters	uniform diameters	a few bead defects	bead defects	heavily beaded fibers

[a)]Maximum dimensions of 3D structure off of collector plate, monitored up to 40 min; [b)]For 3D regions >1 mm in height off collector plate; [c)]Average ± standard deviation (100 fibers/sample).

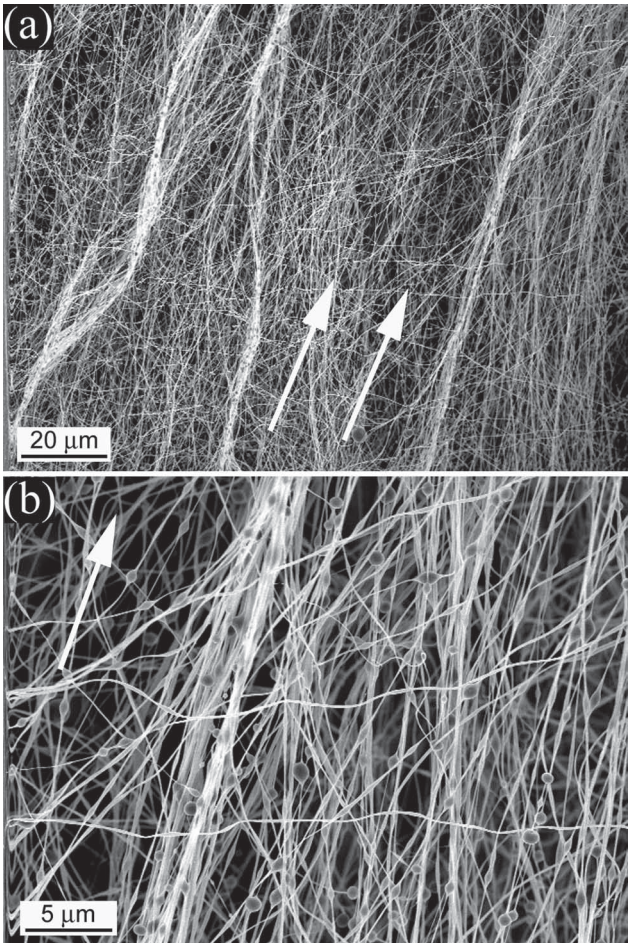

Figure 6. SEM image of a section of a horizontal 'strand' on a 3D electrospun mat (from Figure 5g), prepared by electrospinning an alginate–PEO–F127 solution (10.6:0.8:1.5 wt%) at 23 °C, 40% RH. The arrows indicate the direction of the applied electric field.

3D nanofibrous structures could have potential use as tissue-engineering scaffolds. Another important contribution of this work is that it substantiates the importance of controlling the relative humidity during any electrospinning procedure.

4. Experimental Section

Materials: Sodium alginate was obtained from FMC Biopolymers (Princeton, NJ) and its molecular weight (M_W) was reduced from 196 kDa to 37 kDa by 5 Mrad gamma irradiation (Phoenix Laboratory, University of Michigan, Ann Arbor, MI). Additional details on the irradiation procedure have been previously reported.[37] Polyethylene oxide (M_W 600 kDa, Dow) and Pluronic F127 nonionic surfactant (Sigma Aldrich, St. Louis, MO) were used as received. Solutions containing alginate–PEO (10.6:0.8 wt%) and alginate–PEO–F127 (10.6:0.8:1.5 wt%) were prepared following a procedure previously reported.[35,38] Briefly, alginate and PEO were dissolved into water in separate solutions, and then combined together with F127. Blended solutions were mixed by magnetic stirring for 16–24 h prior to electrospinning.

Solution Characterization: Ionic conductivities of the polymer solutions were measured using a potentiostat (Gamry Instruments) that was calibrated with a 1 mS cm^{-1} potassium chloride standard (Fisher Scientific). Steady-state flow rheological experiments were performed on an AR2000 stress-controlled rheometer (4 cm, 2° cone, TA Instruments, New Castle, DE) at 25 °C. Surface tensions were measured using a pendant drop analyzer from SEO Co. Ltd (model Phoenix 300, Lathes, South Korea).

Electrospinning of 3D Mats: The electrospinning setup consisted of a syringe pump (model NE-1010, New Era Pump Systems, Inc., Wantagh, NY), high-voltage power supply (model AU-60P0.5, Matsusada Precision, Inc. Kusatsu-City, Japan), and a ground collector plate covered with aluminum foil. The solutions were pumped through a syringe with a 22-gauge needle at 0.5 mL h^{-1}. The distance between the needle tip and the collector plate was fixed at 12 cm. During electrospinning, the power supply voltage was adjusted in order to maintain the formation of a Taylor cone on the solution droplet. Timed experiments typically were terminated after 40 minutes. All electrospinning experiments were conducted within a plexiglass glove box to control the ambient conditions. The temperature and relative humidity within the chamber were monitored using a hygrometer (Fisher), and adjusted by flowing dry, compressed air into either an empty or water-filled flask (Figure S3, Supporting Information).

Characterization of Electrospun Mats: The electrospun mats were photographed using a digital SLR camera (EOS Rebel XS,

small 2012,
DOI: 10.1002/smll.201101791

small NANO MICRO

Canon). Video footage was captured with a Sony Handycam camcorder. High-magnification analysis was performed with a FEI XL30 field-emission SEM (6 mm working distance, 5 kV accelerating voltage, spot size 3). The fiber diameters were measured with Adobe Photoshop CS3 on 100 fibers per sample. In addition, surface analyses of the electrospun mats, dried solutions, and neat materials were made using an X-ray photoelectron spectrometer (Kratos Axis Ultra). XPS spectra were calibrated to a C–C peak location at 284.5 eV.

Supporting Information

Supporting Information is available from the Wiley Online Library or from the author.

Acknowledgements

This work was supported by the U.S. Department of Education Graduate Assistance in Areas of National Need (GAANN) Fellowship Program at North Carolina State University (CAB), and a National Science Foundation Graduate Research Fellowship (MDK). The authors gratefully acknowledge fruitful discussions with Professor Alexander Yarin (University of Illinois at Chicago) and Professor Orlin Velev (North Carolina State University) during the preparation of this manuscript.

[1] D. Li, Y. N. Xia, *Adv. Mater.* **2004**, *16*, 1151–1170.
[2] K. Yoon, K. Kim, X. F. Wang, D. F. Fang, B. S. Hsiao, B. Chu, *Polymer* **2006**, *47*, 2434–2441.
[3] L. W. Ji, X. W. Zhang, *Electrochem. Commun.* **2009**, *11*, 1146–1149.
[4] T. H. Cho, T. Sakai, S. Tanase, K. Kimura, Y. Kondo, T. Tarao, M. Tanaka, *Electrochem. Solid-State Lett.* **2007**, *10*, A159–A162.
[5] J. Lee, M. J. Cuddihy, N. A. Kotov, *Tissue Eng. Part B-Reviews* **2008**, *14*, 61–86.
[6] D. Liang, B. S. Hsiao, B. Chu, *Adv. Drug Delivery Rev.* **2007**, *59*, 1392–1412.
[7] N. Bhattarai, Z. S. Li, D. Edmondson, M. Q. Zhang, *Adv. Mater.* **2006**, *18*, 1463–1467.
[8] D. Li, Y. Wang, Y. Xia, *Adv. Mater.* **2004**, *16*, 361–366.
[9] Y. Wang, H. Li, G. Wang, T. Yin, B. Wang, Q. Yu, *J. Nanosci. Nanotechnol.* **2010**, *10*, 1699–1706.
[10] D. M. Zhang, J. Chang, *Nano Lett.* **2008**, *8*, 3283–3287.
[11] B. A. Blakeney, A. Tambralli, J. M. Anderson, A. Andukuri, D. J. Lim, D. R. Dean, H. W. Jun, *Biomaterials* **2011**, *32*, 1583–1590.
[12] L. D. Wright, T. Andric, J. W. Freeman, *Mater. Sci. Eng. C.* **2011**, *31*, 30–36.
[13] T. G. Kim, H. J. Chung, T. G. Park, *Acta Biomaterialia* **2008**, *4*, 1611–1619.
[14] Q. P. Pham, U. Sharma, A. G. Mikos, *Biomacromolecules* **2006**, *7*, 2796–2805.
[15] R. Gentsch, B. Boysen, A. Lankenau, H. G. Borner, *Macromol. Rapid Commun.* **2010**, *31*, 59–64.
[16] H. G. Sundararaghavan, R. B. Metter, J. A. Burdick, *Macromol. Biosci.* **2010**, *10*, 265–270.
[17] S. Srouji, T. Kizhner, E. Suss-Tobi, E. Livne, E. Zussman, *J. Mater. Sci.: Mater. Med.* **2008**, *19*, 1249–1255.
[18] H. Okuzaki, T. Takahashi, N. Miyajima, Y. Suzuki, T. Kuwabara, *Macromolecules* **2006**, *39*, 4276–4278.
[19] P. C. Hiemenz, R. Rajagopalan, *Principles of Colloid and Surface Chemistry*, 3rd ed., Marcel Dekker, New York, NY **1997**.
[20] X.-Y. Sun. *Concurrent and Sequential Surface Modification of Electrospun Polymer Micro/Nano Fibers*, PhD Dissertation, North Carolina State University, Raleigh, NC **2008**.
[21] X. Y. Sun, R. Shankar, H. G. Borner, T. K. Ghosh, R. J. Spontak, *Adv. Mater.* **2007**, *19*, 87–91.
[22] S. Tripatanasuwan, Z. X. Zhong, D. H. Reneker, *Polymer* **2007**, *48*, 5742–5746.
[23] C. L. Pai, M. C. Boyce, G. C. Rutledge, *Macromolecules* **2009**, *42*, 2102–2114.
[24] C. L. Casper, J. S. Stephens, N. G. Tassi, D. B. Chase, J. F. Rabolt, *Macromolecules* **2004**, *37*, 573–578.
[25] A. L. Yarin, S. Koombhongse, D. H. Reneker, *J. Appl. Phys.* **2001**, *89*, 3018–3026.
[26] M. F. Durstock, M. F. Rubner, *Langmuir* **2001**, *17*, 7865–7872.
[27] N. A. M. Barakat, M. A. Kanjwal, F. A. Sheikh, H. Y. Kim, *Polymer* **2009**, *50*, 4389–4396.
[28] S. J. Kim, S. G. Yoon, Y. H. Lee, S. I. Kim, *Polymer Int.* **2004**, *53*, 1456–1460.
[29] C. A. Bonino, L. Ji, Z. Lin, O. Toprakci, X. Zhang, S. A. Khan, *ACS Appl. Mater. Interfaces* **2011**, *3*, 2534–2542.
[30] D. H. Reneker, A. L. Yarin, *Polymer* **2008**, *49*, 2387–2425.
[31] E. Zussman, A. Theron, A. L. Yarin, *Appl. Phys. Lett.* **2003**, *82*, 973–975.
[32] D. Li, Y. L. Wang, Y. N. Xia, *Nano Lett.* **2003**, *3*, 1167–1171.
[33] F. Bordi, C. Cametti, R. H. Colby, *J. Phys.: Condens. Matter* **2004**, *16*, R1423–R1463.
[34] H. Fong, I. Chun, D. H. Reneker, *Polymer* **1999**, *40*, 4585–4592.
[35] C. A. Bonino, M. D. Krebs, C. D. Saquing, S. I. Jeong, K. L. Shearer, E. Alsberg, S. A. Khan, *Carbohydr. Polym.* **2011**, *85*, 111–119.
[36] C. A. Bonino, *Functional Nanofibers and Hydrogels: From Energy Storage to Biomedical Applications*, PhD Dissertation, North Carolina State University, Raleigh, NC **2011**.
[37] E. Alsberg, H. J. Kong, Y. Hirano, M. K. Smith, A. Albeiruti, D. J. Mooney, *J. Dental Res.* **2003**, *82*, 903–908.
[38] S. I. Jeong, M. D. Krebs, C. A. Bonino, S. A. Khan, E. Alsberg, *Macromol. Biosci.* **2010**, *10*, 934–943.

Received: September 1, 2011
Revised: January 5, 2012
Published online: